DESIGN AND PERFORMANCE ANALYSIS OF A THREE WINDING TRANSFORMER USED IN SOLAR SYSTEM

A. Jahi [1,3]   I. Iskender [2]

1. Electrical and Electronics Engineering Department, Gazi University, Ankara, Turkey, amir.jahi@gazi.edu.tr
2. Electrical and Electronics Engineering Department, Cankaya University, Ankara, Turkey, ires@cankaya.edu.tr
3. SEM Transformer Inc., Ankara, Turkey

Abstract- Due to the increasing of the fossil fuels prices in the past years and lack of these sources, all scientists encouraged to looking for the alternative energy sources. One of these energy sources is the renewable solar resources. Power transfer from solar systems to grid is achieved using step up transformers. This type of transformer is energized from a converter/inverter with or without variable frequency. The losses of such transformer are higher than those used in sinusoidal voltage power systems. This is due to harmonics content in the transformer input voltage and current. In this study the design and production of a PV transformer have been done according to the IEEE C57.159 guide and the loss analyses of transformer have been done using ANSYS MAXWELL considering the procedures proposed in standards of IEC 61378-1, IEEE C57.110 and the method proposed by Dowell. Finally, the thermal modeling and behavior of the transformer was investigated using the thermal model given in [25] to determine the hot spot and life time of the transformer using MATLAB program.

Keywords: PV (Photovoltaic), High Frequency (HF), Finite Element Method (FEM), Eddy Loss, Transformer.

1. INTRODUCTION

Power transformer is one of the most important equipment in the energy transmission systems. Precise calculation of the operation losses of a large power transformer plays an important role in the design process. One of the difficult stages in transformer design is calculation of the stray losses in transformer. Eddy current losses increase with increase in frequency causing increase in winding losses of transformer. The operating temperature of transformer increases depending on the power losses. The exact calculation of the winding losses for different operating frequency and winding geometry is necessary for electrical and cost optimization.

In this respect, precise prediction and calculation of high frequency eddy current loss in winding including winding skin and proximity effect are very important. It is hard to get a general analytical method for calculation of the high frequency eddy current in winding because of the transformer active part and winding complexity. In recent years, several approaches have been used for calculation of the related losses in round winding type of transformer as reviewed in [1].

One of the analytical methods which is used for calculation of high frequency eddy current losses for foil type winding of transformer is the Dowell method through which the total thickness and cross section of the round winding are converted to the equivalent foil winding [2-6]. Ferreira uses the single round conductor with a uniform field in his method which called Bessel-function method [7-11]. The mentioned methods can get wrong result at high frequency operation [12]. The most commonly method used for calculation of winding eddy losses for any winding geometry and winding configuration is Finite Element Method.

This paper employs transient Finite Element Method for modeling and simulation of 5.1 MVA 60 Hz with concentric winding configuration PV Transformer by providing field analysis which is more accurate method of analysis and simulation of transformer. Then, the high frequency power loss of PV transformer has been calculated based on IEC 61378-1 standard and simulation results.

2. DESIGN OF THE PV TRANSFORMER

In this study, a 3-phase, Dyn11yn11, 5.1 MVA, 34.5/0.66-0.66 kV three concentric winding transformer with two 2550 kVA low voltage winding is considered to be designed. The transformer is fed through two separate inverters and Figures 1 and 2 show the winding configuration of the considered transformer.
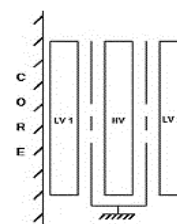

Figure 1. Winding configurations of the three-winding transformer

Figure 2. Winding configurations of the three-winding transformer

The design of the conventional transformer begins with the design of the active part of the transformer which consists of the core section, magnetic flux density, high voltage and low voltage turn number and the current density of the conductor. The design of the transformer tank and cooling walls is achieved by calculating the amount of the losses which should be dissipated by heat transfer. The design specification of the subjected transformer is shown in Table 1.

Table 1. Transformer specification

Manufacturer	SEM	
Model	5.1 MVA, 34.5/0.66-0.66 kV, 60 Hz	
Secondary rated current (A)	85.35	
Primary rated current (A)	2230.6	
Vector group	Dyn11yn11	
Primary turn numbers	13	
Primary conductor (mm)	AL-710x1.6	
Secondary Turn numbers	1177	
Secondary conductor (mm)	AL-9.7x2.6	
Maximum flux density	1.65 T	
Core cross section (mm²)	66.76	
Core Yoke distance (mm)	1458	
Core Leg distance (mm)	1048	
Load Loss (W)	Low Voltage 1 DC	8025
	Low Voltage 2 DC	14140
	High Voltage DC	20194
	Stray Loss	4583
	Total	46942
No load losses (W)	3613	

3. TRANSFORMER MODEL AND SIMULATION

The PV transformer considered in this study is a 3-phase concentric, Dyn11yn11, 5.1 MVA, 34.5/0.66-0.66 kV with one HV winding positioned radially between the two LV_1 and LV_2 windings. In Figures 3 and 4 the three- and two-dimensional models of the PV transformer with necessary meshes are shown. The brief technical specification of the transformer is demonstrated in Table 1.
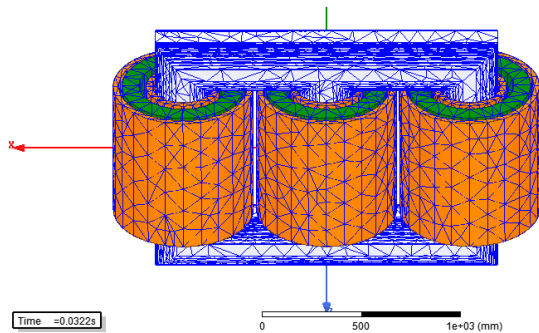

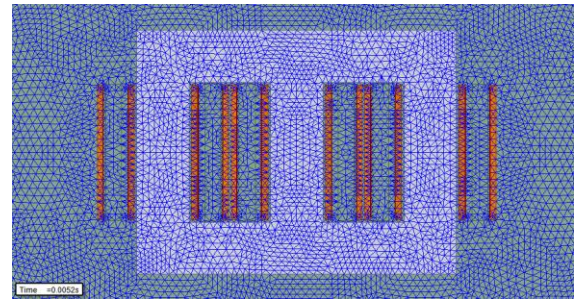Figure 3. 3D meshing model of the PV transformer

Figure 4. 2D meshing model of the PV transformer

According to the simulation result, the voltage and current transient report of the secondary (High voltage) and primary (Low voltage) winding are given in Figures 5-8.
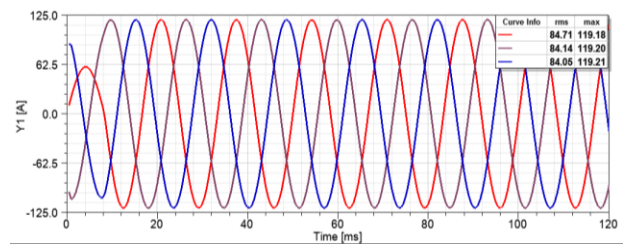

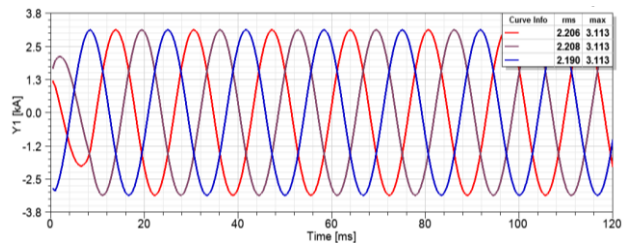Figure 5. Secondary winding current
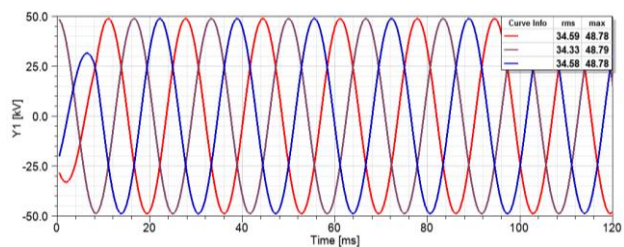

Figure 6. Primary windings current
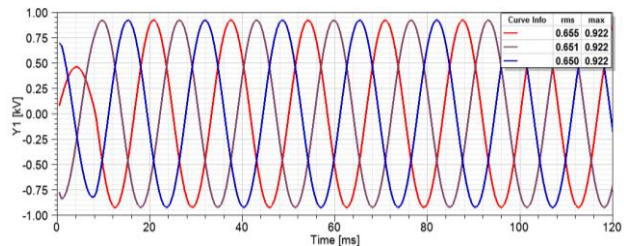

Figure 7. Secondary winding voltage 2

Figure 8. Primary windings voltage

Figure 9 shows no-load loss of studied transformer versus time. The core magnetic flux density distribution is show on 2D and 3D model in Figures 10 and 11. The magnetic flux density waveform is shown in Figure 12.
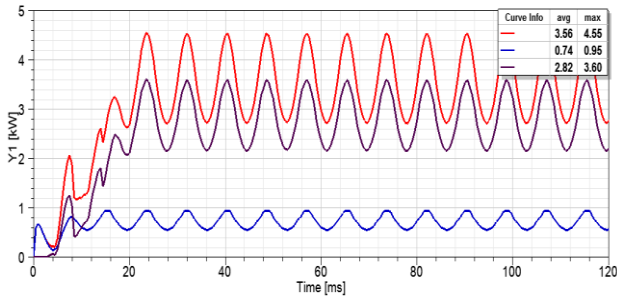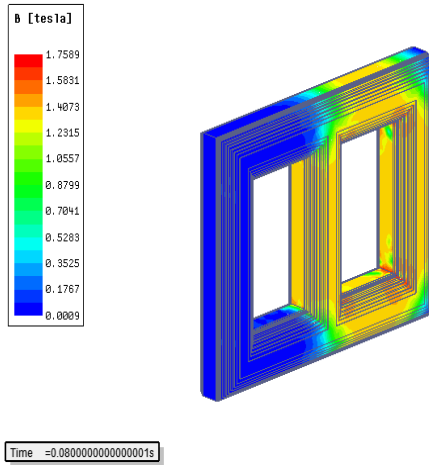
Figure 9. No load loss
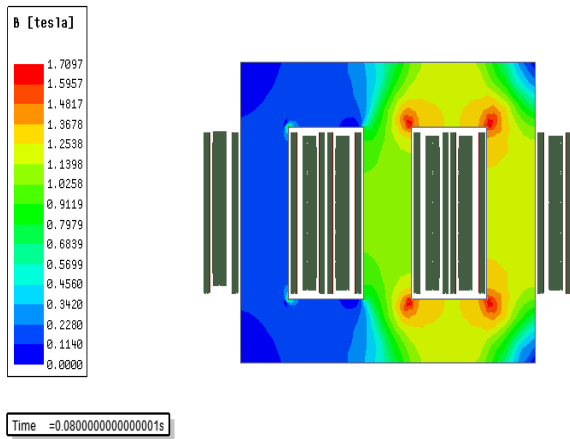

Figure 10. Magnetic flux density (3D)
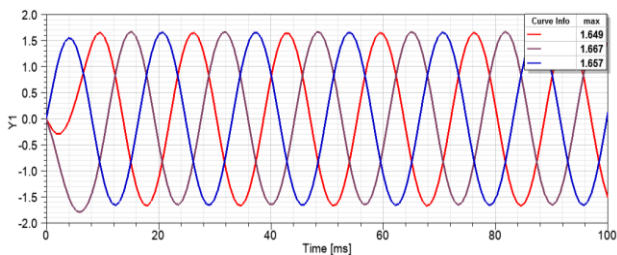

Figure 11. Magnetic flux density (2D)

Figure 12. Magnetic flux density waveform

The ohmic loss of each winding of the studied transformer obtained as a result of the simulation are shown in Figures 13-15.
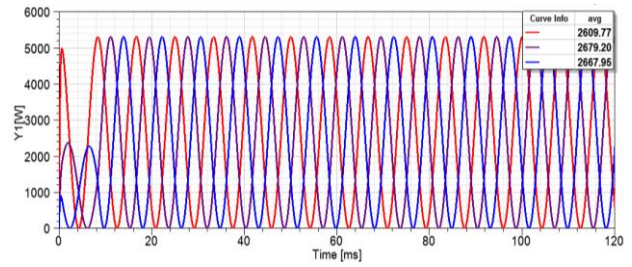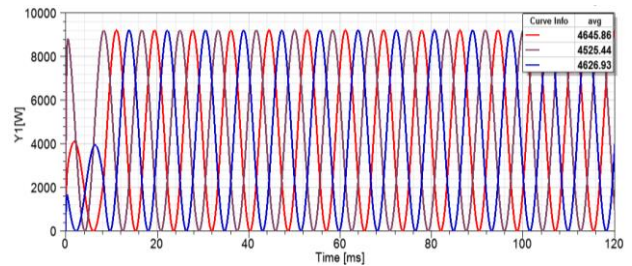

Figure 13. Ohmic loss of LV$_1$ winding

Figure 14. Ohmic loss of LV$_2$ winding
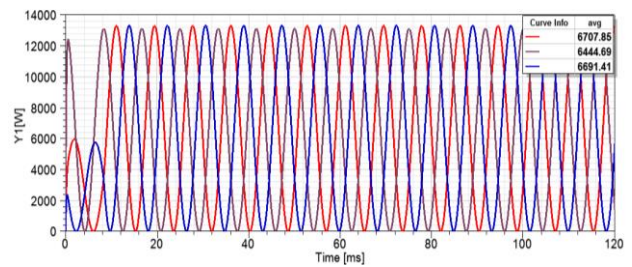
Figure 15. Ohmic loss of HV winding

4. DETERMINATION OF TRANSFORMER LOAD LOSS UNDER DISTORTED CURRENTS

The load losses of the transformer consist of the winding DC losses and stray losses which subdivided to the eddy current loss of the conductors and connections and stray losses in the metal part of the transformer like core clamps, tank and cover.

In such transformer that the low voltage winding current is about kA level the additional calculation and analysis of the losses that appear in the phase and bushing connections should also be considered. The following principles are used in this paper:

The eddy current losses of the winding connections and metallic shields such as copper or aluminum are linear and in accordance with:

$$P(I) = \text{CONSTANT} \times I^2$$

a similar relationship is also valid for shields of magnetic core steel, when used in unsaturated conditions:

$$P(B) = \text{CONSTANT} \times B^2$$

for the stray losses in structural steel parts, a square law relationship may also be used with reasonable accuracy where, $B^2 = \text{CONSTANT} \times I^2$

The load current of the PV transformer is non sinusoidal because of the high frequency harmonics generated by converter/inverter. These harmonic currents cause additional losses than the normal service operation or with sinusoidal wave current which result to increasing

the total losses and causes overheating of the transformer. For this reason, precise prediction and calculation of these additional losses which represent the transformer correct service condition should be taken into account at sizing of the transformer.

The thermal dimensioning of the transformer shall be in accordance with the operational rated harmonic load current components confirmed by the costumer. A few years ago, suppliers may calculate the current harmonic component according to 5.5 of IEC/TR 60146-1-2:2011. However, recent developments in electronics make possible the application of real-time control techniques that significantly alter the behavior of the converter. The result is that a clear relationship between the converter power circuit configuration and its number of pulses, and hence the value of the current harmonics, is uncertain and the actual current harmonics may differ significantly from those computed according to 5.5 of IEC/TR 60146-1-2.

In any case the current harmonic components to be used for the design of the transformer shall be clearly defined and indicate in the technical sheets of the purchase order. The following rules are given for the recalculation of the measured loss under test to the loss value valid under the specified converter loading [19, 20].

Total loss with distorted current is calculate by:

$$P_N = I_{LN}^2 \times (R_W + R_C) + (F_{WE} \times P_{WE1}) + F_{CE} \times (P_{CE1} + P_{SE1}) \quad (1)$$

The enhancement factor for connections is equal to

$$\sum_1^n \left(\frac{I_h}{I_1}\right)^2 \times h^{0.8} = F_{CE} \quad (2)$$

As given in [19, 20], the enhancement factor for the stray loss in structural parts is taken as equal to that of bus bar systems.

$$F_{CE} = P_{SE} / P_{SE1} = F_{CE} \quad (3)$$

A more accurate estimate of the eddy loss enhancement factor for windings, F_{WE}, can be made if the winding eddy loss components from axial and radial stray flux, P_{WEax1} and P_{WErad1} respectively, are known. These will be calculated at fundamental frequency using a finite element method of field analysis.

Since the distribution of the harmonic stray flux is the same as that of the flux at fundamental frequency in conventional windings consisting of individual strands, the following relationships may be derived. Relation between strand dimensions and penetration depths is:

$$X_{ah} = t \times \left(\frac{\mu_r \times \mu_r \times w_1 \times h}{2 \times \rho}\right)^{0.5} \quad (4)$$

$$X_{rh} = l \times \left(\frac{\mu_r \times \mu_r \times w_1 \times h}{2 \times \rho}\right)^{0.5} \quad (5)$$

Hence, the expression for the winding enhancement factor F_{WE} may be expressed as:

$$F_{WE} = \frac{P_{WEax1}}{P_{WE1}} \times \sum_1^n \left(\frac{I_h}{I_1}\right)^2 \times \frac{\psi(X_{ah})}{\psi(X_1)} +$$
$$+ \frac{P_{WErad1}}{P_{WE1}} \times \sum_1^n \left(\frac{I_h}{I_1}\right)^2 \times \frac{\psi(X_{rh})}{\psi(X_1)} \quad (6)$$

where,

$$\psi(X_h) = 2X_h \times \frac{\sinh X_h - \sin X_h}{\cosh X_h + \cos X_h} \quad (7)$$

For foil windings the winding enhancement factor may be taken as:

$$F_{WE} = \frac{P_{WEax1}}{P_{WE1}} \times \sum_1^n \left(\frac{I_h}{I_1}\right)^2 \times h^2 +$$
$$+ \frac{P_{WErad1}}{P_{WE1}} \times \sum_1^n \left(\frac{I_h}{I_1}\right)^2 \times h^{0.5} \quad (8)$$

Eddy losses could be derived for layers of winding from Equation (9) [21],

$$P = 2I^2 \frac{\rho(ALW)N^2}{h\delta p\eta} \left[\frac{\sinh(2\Delta)+\sin(2\Delta)}{\cosh(2\Delta)-\cos(2\Delta)}\right] +$$
$$+ \frac{2}{3}(p^2 - 1)\left[\frac{\sinh(\Delta)-\sin(\Delta)}{\cosh(\Delta)+\cos(\Delta)}\right] \quad (9)$$

where, I is the rms value of the current, N represent the turn number, the total layers is p, the average length of winding is ALW, η is the ratio of conductor thickness to distance between adjacent conductor which assumed 0.9 in this paper and Δ is the penetration ratio.

The axial and radial losses used to evaluate winding eddy current losses are calculated by,

$$P_a = \frac{B_y^2 W^2 \sigma t^2}{24} \quad (10)$$

$$P_r = \frac{B_x^2 W^2 \sigma l^2}{24} \quad (11)$$

where, P_a and P_r is the axial and radial losses of the winding respectively [22]. In this equation By and Bx are the peak magnetic flux which are obtained from the FEM analysis. Figures 16-18 show the leakage axial and radial flux density in the area and flux density in the windings, respectively.
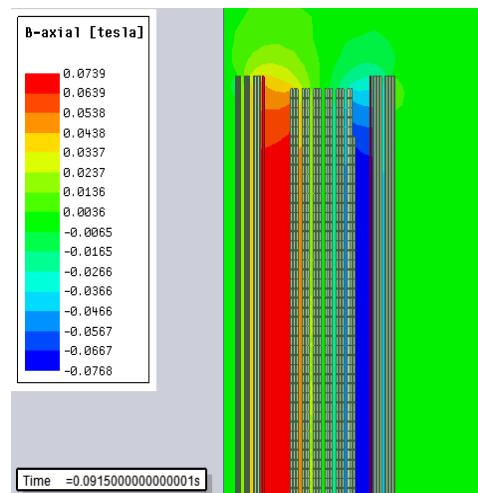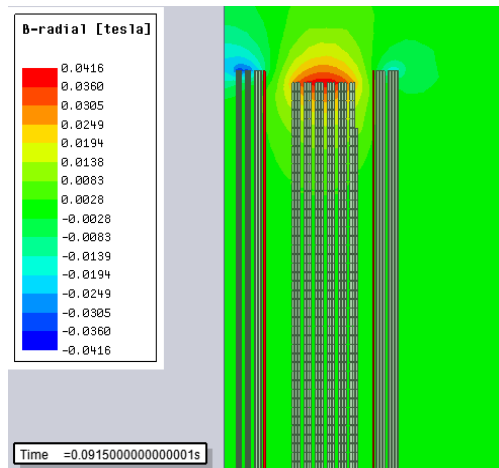

Figure 16. Axial flux density
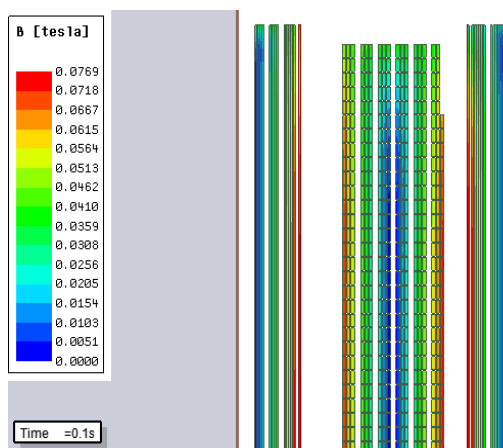
Figure 17. Radial flux density

Figure 18. Flux density in the windings

5. SIMULATION RESULTS

The detailed harmonic content of the primary current generated by the PWM converters is shown in Table 2. The load loss analysis has been done based on the design specification, FEM analyses data and factory test results.

Table 2. High frequency harmonic content

Frequency (Hz)	Value (%)
60	100%
120	0.273
300	0.170
420	0.170
780	0.175
4520	0.311
4520	0.412
4760	0.398
4880	3.208
5120	3.144
5240	0.379
5480	0.396
5600	0.289
9580	0.313
9940	0.838
10060	0.789
10420	0.321
14760	0.321
14880	0.558
15120	0.252
15240	0.208
THD	4.85

The total eddy and dc losses on each layer of the low voltage winding obtained from axial and radial flux distributions are given in Table 3. There are 13 layers in each winding and the loss analysis was performed for different frequencies including fundamental and harmonic content.

Table 3. Low voltage winding load losses calculation results with FEM

Layer	60 (Hz)		4.8 (kHz)		5.12 (kHz)	
	LV_1	LV_2	LV_1	LV_2	LV_1	LV_2
1	148	330	1.5	20	1	27
2	149	327	2	16	1.5	23
3	151	324	2.2	15	2	17
4	156	323	2.5	13	3.1	14
5	158	319	2.7	11	3.5	11
6	159	321	3.6	10	4	8.5
7	161	322	5.4	8	5	7.6
8	167	320	6.2	7.1	6.9	6
9	169	318	7.1	6	8	5
10	170	317	7.5	5.3	9.9	4.1
11	172	315	9	4.5	10.9	3
12	174	316	10	3.6	12	2.5
13	176	313	13	3	14	2
Total Losses (W)	2111	4165	73	122	82	131

Table 4 shows the results of load losses calculated by the axial and radial leakage flux on each layer of HV winding which consists of 66 strands of rectangular wire in each layer and 55 strands in last layer at rated frequency and HF respectively. The following conclusion can be made from the calculated results and Figure 18;

1. At LV_1, losses at last layers is higher than the losses of the first layers
2. At LV_2, losses at first layers is higher than the losses of the last layers
3. At HV, Losses in the middle of the winding is lower than the losses of the first and last layers.

Table 4. High voltage winding load losses calculation results with FEM

Layer	60 (Hz)	4.8 (kHz)	5.12 (kHz)
	HV	HV	HV
1	324	47	40
2	325	40	37
3	333	28	30
4	326	27	29
5	340	25	24
6	349	21	22
7	354	18	19
8	358	19	18
9	368	19	18
10	372	17	18
11	376	19	21
12	386	22	24
13	390	24	26
14	394	29	32
15	407	45	43
16	412	51	46
17	418	56	55
18	344	31	29
Total Losses (W)	6588	536	530

As shown in Table 5, the calculated total load loss of the PV transformer is 52.4 kW which increases about 5.5 kW under the distorted current condition because of the high frequency current harmonics.

Table 5. HF losses calculation results with IEC method

	HV	LV$_2$	LV$_1$
I_{LN} (A)	85.44	2233.26	2233.26
R_W (mΩ)	2640	0.83	0.42
R_C (mΩ)	150	0.11	0.12
$P_{winding\ eddy}$ (W)	534.6	164.5	82.5
F_{WE}	4.8	12.80	12.64
P_{WE1} (W)	534.51	164.54	82.48
P_{WEAX1} (W)	180.9	84.98	43.66
P_{WERAD1} (W)	361.81	146.51	35.71
F_{CE}	1.09		
$P_{CE1} + P_{SE1}$ (W)	3801.47		
$P_{Total\ Load\ Loss}$ (W)	52445		

Table 6 illustrate the calculated high frequency losses according to the IEC standard, IEEE standard, Modified Dowell method and FEM.

Table 6. HF losses calculation results

	IEC	FEM	Dowell	IEEE
$P_{Total\ Load\ Loss}$ (W)	52445	52685	54204	64569

It is seen from Table 6 that the losses corresponding to methods indicated in Table are different and the losses of IEEE Standard is greater than the others. Considering the cooling problem of transformer, the tank dimension and cooling area of transformer with higher losses should be large enough to satisfy cooling conditions.

6. THERMAL MODEL

One of the most dangerous problems of the transformer is the high temperature of the transformer in the field. The operating temperature higher than the design value causes a degradation of the insulation and fault of the transformer. In this paper the thermal model of the transformer under distorted current has been done using MATLAB program. For the modeling of top oil and hot spot temperature of the transformer the thermal model of the SUSA was used [25]. The difference of this method with those of IEC and IEEE methods is that in this model the change of the oil viscosity with the temperature is taken into account. The calculated load losses for HF harmonics with the ambient temperature varying from 25 to 49 degree during one sunny day is shown in Figure 20.

The top oil and hot spot temperature can be obtained from Equations (12) and (13), respectively.

$$\frac{1 + R \times P_{l,pu} \times K^2}{1 + R} \times \mu_{pu}^n \times \Delta\theta_{oil.rated} =$$
$$= \mu_{pu}^n \times \tau_{oil,rated} \times \frac{d_{oil}^\theta}{dt} + \frac{(\theta_{oil} - \theta_{amb})^{1+n}}{\Delta\theta_{oil,rated}^n} \quad (12)$$

$$\{K^2 \times P_{wdn,pu}(\theta_{hs})\} \times \mu_{pu}^n \times \Delta\theta_{hs,rated} =$$
$$= \mu_{pu}^n \times \tau_{wdn,rated} \times \frac{d\theta_{hs}}{dt} + \frac{(\theta_{hs} - \theta_{oil})^{1+n}}{\Delta\theta_{hs,rated}^n} \quad (13)$$

where, n is the top oil and hot spot constant which is equal to 0.25 for the ONAN transformer and R is the ratio of rated load losses to the no load losses.
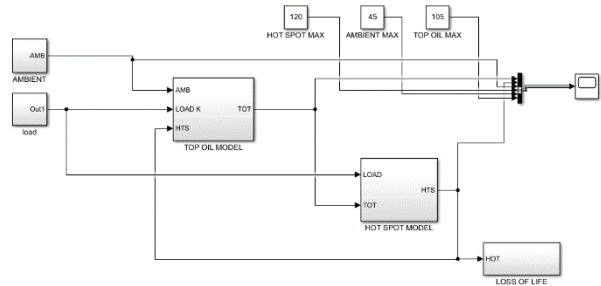

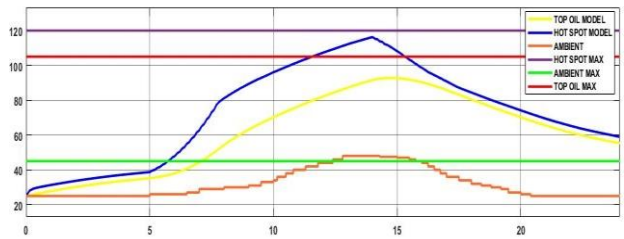Figure 19. Block diagram of the thermal model

Figure 20. Thermal modeling result

Table 7 illustrates the analysis results of the thermal modeling of the transformer under distorted currents. The design of the tank and cooling wall of the transformer has been done considering the increase amount of the load losses in the field operation.

Table 7. Analysis results of the thermal modeling

	Design Value (°C)	Analysis Result (°C)
Max. Ambient	45	49
Max. Top Oil	105	97
Max. Top Oil Rise	55	48
Max. Hot Spot	120	113

The relative ageing rate for thermally upgraded paper and loss of life calculation of the transformer are defined according to Equations (14) and (15), respectively [26].

$$V = e^{\left(\frac{15000}{110+273} - \frac{15000}{\theta_{hs}+273}\right)} \quad (14)$$

$$L = \int^t V dt \quad (15)$$

Figure 21 shows the loss of life calculation of the transformer under HF harmonics. In simulation the ambient temperature is assumed to be higher than the design value at some hours for showing the effect of the higher hot spot values on the life of the transformer. It is seen from the figure that the life time of the transformer decreases about 96.5% of the normal life time of the transformer and this is due to effect of higher ambient temperature which is greater than the design value.
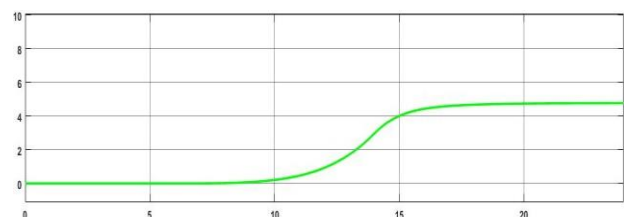

Figure 21. Calculated loss of life of the transformer

6. CONCLUSIONS

In this paper, a 3-phase, Dyn11yn11, 5.1 MVA, 34.5/0.66-0.66 kV PV transformer which energized from a converter/inverter with non-sinusoidal voltage was investigated to determine and calculate of HF losses. Finite element method is used to show 3D and 2D models of the subjected transformer regarding to presents field behavior of the transformer. It has been known that, the converter transformer load current is non-sinusoidal and has a number of harmonic currents with noticeable size causing increase in load losses and temperature of the transformer. In design process the (i.e., number of layers, thickness of conductors, etc.) the presence of the HF harmonics should be considered to maintain the internal losses and temperature rise of the transformer in safe levels. In this sense, design of the transformer and calculation of the power losses by means of FEM, as described in EN/IEC 61378-1 may be recommended. Sizing of the transformer using direct application of harmonic loss factor will lead to oversized design where calculated losses are normally much higher than the real field losses.

NOMENCLATURES

1. Symbols / Parameters

I_{LN} : I_L at rated converter load

I_L : Current r.m.s. value of low voltage winding

R_W : Resistance value of conductors

R_C : Resistance value of connections

P_{WE1} : Winding eddy loss with current I_1

P_{CE1} : Connection eddy loss with current I_1

P_{SE1} : Structural parts stray loss with current I_1

F_{WE} : Eddy loss enhancement factor for windings

F_{CE}: Eddy loss enhancement factor for connections

F_{SE}: Stray loss enhancement factor for structural parts

$W1$: The pulse of fundamental frequency

h: The harmonic order

μ_0: The permeability of vacuum

μ_r: The relative permeability

σ: Conductivity

w: Angular frequency

t: Thickness of the winding

l: Height of the winding

$P_{l,pu}$: Rated load losses of the transformer

$\Delta\theta_{oil.rated}$: Rated top oil temperature rise

μ_{pu}: Oil viscosity

$\tau_{oil,rated}$: Rated oil time constant

θ_{oil} : Rated top oil temperature

θ_{amb} : Ambient temperature

$\tau_{wdn,rated}$: Rated winding time constant

θ_{hs} : Rated hot spot temperature

$\Delta\theta_{hs,rated}$: Rated hot spot temperature rise

$P_{wdn,pu}$: Rated winding losses

K: Load factor

REFERENCES

[1] G.R. Skutt, T.G. Wilson, A.M. Urling, V.A. Niemela, "Characterizing High-Frequency Effects in Transformer Windings - A Guide to Several Significant Articles", Journal of Circuits, Systems, and Computers, Vol. 5, Dec. 1996.

[2] P.L. Dowell, "Effects of Eddy Currents in Transformer Windings", Proceedings of the IEE, Vol. 113, No. 8, pp. 1387-1394, Aug. 1966.

[3] P.S. Venkatraman, "Winding Eddy Current Losses in Switch Mode Power Transformers due to Rectangular Wave Currents", Proceedings of Powercon 11, Power Concepts Inc., pp. 1-11, 1984.

[4] M.P. Perry, "Multiple Layer Series Connected Winding Design for Minimum Losses", IEEE Transactions on Power Apparatus and Systems, Vol. PAS-98, pp. 116-123, Jan./Feb. 1979.

[5] E. Bennet, S.C. Larson, "Effective Resistance of Alternating Currents", American Institute of Electrical Engineers, Vol. 59, pp. 1010-1017, 1940.

[6] R.L. Stoll, "The Analysis of Eddy Currents", Clarendon Press, Oxford, 1974.

[7] J.A. Ferreira, "Improved Analytical Modeling of Conductive Losses in Magnetic Components", IEEE Transactions on Power Electronics, Vol. 9, No. 1, pp. 127-31, Jan. 1994.

[8] M. Bartoli, N. Noferi, A. Reatti, M.K. Kazimierczuk, "Modeling Litz-Wire Winding Losses in High-Frequency Power Inductors", The 27th Annual IEEE Power Electronics Specialists Conference, Vol. 2, pp. 1690-1696, June 1996.

[9] W.R. Smythe, "Static and Dynamic Electricity", McGraw-Hill, p. 411, 1968.

[10] J.A. Ferreira, "Analytical Computation of AC Resistance of Round and Rectangular Litz Wire Windings", IEE Proceedings-B Electric Power Applications, Vol. 139, No. 1, pp. 21-25, Jan. 1992.

[11] J.A. Ferreira, "Electromagnetic Modelling of Power Electronic Converters", Kluwer Academic Publishers, 1989.

[12] X. Nan, C.R. Sullivan, "An Improved Calculation of Proximity Effect Loss in High Frequency Windings of Round Conductors", PESC03, Vol. 2, pp. 853-860, 2003.

[13] C.R. Sullivan, "Computationally Efficient Winding Loss Calculation with Multiple Windings, Arbitrary Waveforms, and Two- or Three Dimensional Field Geometry", IEEE Transactions on Power Electronics, Vol. 16, No. 1, pp. 142-150, Jan. 2001.

[14] A.D. Podoltsev, "Analysis of Effective Resistance and Eddy Current Losses in Multi Turn Winding of High-Frequency Magnetic Components", IEEE Transactions on Magnetics, Vol. 39, No. 1, pp. 539-548, Jan. 2003.

[15] E.C. Snelling, "Soft Ferrites, Properties and Applications", Butterworths, The Second Edition, 1988.

[16] C.R. Sullivan, "Optimal Choice for Number of Strands in a Litz Wire Transformer Winding", IEEE Transactions on Power Electronics, Vol. 14, No. 2, pp. 283-291, 1999.

[17] J.H. Spreen, "Electrical Terminal Representation of Conductor Loss in Transformers", IEEE Transactions on Power Electronics, Vol. 5, No. 4, pp. 424-9, 1990.

[18] P. Meesuk "Magnetic Field Analysis for a Distribution Transformer with Unbalanced Load Conditions by using 3-D Finite Element Method", World Academy of Science, Engineering and Technology 60, 2011.

[19] IEC 61378-1, "Converter Transformers - Part 1: Transformers for Industrial Applications", Edition 2.0, 2011-07.

[20] IEC 61378-3, "Converter Transformers - Part 3: Application Guide", Edition 2.0, 2015-02.

[21] K. Iyer, "Transformer Winding Losses with Round Conductors and Foil Windings for Duty-Cycle Regulated Square Waveform Followed by Winding Design and Comparison for Sinusoidal Excitation", University of Minnesota, 2013.

[22] M. Cyril Hlatshwayo, "The Computation of Winding Eddy Losses in Power Transformers Using Analytical and Numerical Methods", University of the Witwatersrand, 2011.

[23] M.Z. Zahedi, I. Iskender, "3D FEM Optimal Design of Transformer Cover Plates to Decrease Stray Losses and Hot Spot Temperature", International Journal on Technical and Physical Problems of Engineering (IJTPE), Issue 28, Vol. 8, No. 3, pp. 56-60, September 2016.

[24] M.Z. Zahedi, I. Iskender, "FDM Electromagnetic Analysis in Bushing Regions of Transformer", International Journal on Technical and Physical Problems of Engineering (IJTPE), Issue 34, Vol. 10, No. 1, pp. 27-33, March 2018.

[25] D. Susa, M. Lehtonen, H. Nordman, "Dynamic Thermal Modelling of Power Transformers", IEEE Trans. Power Delivery, Vol. 20, pp. 197-204, 2005.

[26] IEC 60076-7, "Loading Guide for Oil-Immersed Power Transformers", IEC standard, 60076-7,1-84, 2018.

BIOGRAPHIES

Amir Jahi received his M.Sc. degree in Electrical and Electronic and Electronics Engineering in 2013, from the University of Gazi, Ankara, Turkey. He is currently a Ph.D. student in electrical engineering at the same university. Generally, he is interested in researching about transformers and power electronics.

Ires Iskender received his Ph.D. degree in Electrical and Electronics Engineering from Middle East Technical University (Ankara, Turkey) in 1996. Prior to joining the Department of Electrical and Electronics Engineering of Cankaya University (Ankara, Turkey), he worked as a Professor at Department of Electrical and Electronics Engineering in Middle East Technical University and Gazi University. His current research interests are energy conversion systems, renewable energy sources, electrical machine and power quality. He participated in and coordinated several research projects and he served as the panelist and referee for many academic or industry projects.